Numerical Simulation of Radiant Ceiling Systems for Determining the Parameters Affecting Cooling Capacity

Mina Alafzadeh[1], and Mehran Rabani[1,*]

[1] Department of Mechanical Engineering, Faculty of Engineering, Ardakan University, Ardakan, P.O. Box 184, Iran
*Corresponding authors, Email: m.rabani@ardakan.ac.ir

Manuscript received 18 April, 2026; revised 18 July, 2026; accepted 15 August, 2026. Paper no. JEMT-2604-1590.

This study presents a three-dimensional numerical simulation of chilled water flow in copper pipes installed on an aluminum plate using ANSYS Fluent to optimize the thermal performance of radiant ceiling panels. Unlike previous studies that have examined design parameters in isolation, the present work simultaneously investigates the coupled effects of four key variables pipe spacing, pipe diameter, mass flow rate, and inlet fluid temperature on cooling capacity and surface temperature uniformity. The flow was modeled as turbulent, incompressible, and transient, and the numerical model was validated against ASHRAE experimental data. The results show that reducing tube spacing from 0.30 m to 0.05 m increases cooling capacity by up to 35%; a practical range of 10–15 cm (60–63 W) is recommended. Reducing pipe diameter from 20 mm to 10 mm yields an 8% performance gain, with 12 mm (102 W) identified as the practical optimum. Increasing mass flow rate raises cooling capacity by 25%, with a pronounced step increase at the laminar-to-turbulent transition (0.016–0.017 kg/s). Inlet temperature exerts the largest influence, with capacity ranging from 108 W at 12 °C to 46 W at 18 °C; 15 °C is recommended as the optimal operating point. Transient analysis confirms that the panel reaches thermal steady state within approximately 3 minutes significantly faster than concrete-embedded alternatives. The coupled parametric framework provides a systematic basis for the component-level design of energy-efficient radiant cooling systems, advancing beyond prior single-parameter studies by quantifying the interactions among geometric, hydraulic, and thermal design variables within a unified model.

Keywords: *Radiant ceiling panels, Cooling capacity, ANSYS Fluent software, Transient flow, Turbulent flow*.

http://dx.doi.org/10.22109/jemt.2026.579055.1590

Nomenclature

Latin Symbols

Symbol	Definition	Unit
b	Total width of pipe array	m
C_o	Courant number	—
c_p	Specific heat capacity of fluid	J/kg·K
D	Pipe inner diameter	m
fi	External body force per unit volume in *i*-th direction	N/m³
k	Thermal conductivity	W/m·K
l	Tube length	m
P	Static pressure	Pa
q	Heat flux	W/m²
Q	Inlet mass flow rate	kg/s
Re	Reynolds number	—
s	Tube center to center spacing	m
S_h	Volumetric energy source term	W/m³
t	Time	s
T	Temperature	K
ui , uj	Velocity components in *i*- and *j*-directions	m/s
xi , xj	Cartesian coordinate directions	m
y^+	Dimensionless wall distance	—

Greek Symbols

Δh	Spatial step size (mesh element size)	m
Δt	Time step	s
μ	Dynamic viscosity	Pa·s
ρ	Fluid (water) density	kg/m³
Φ	Viscous dissipation function	W/m³

Subscripts

i	Inlet condition
m	Mean panel surface
r	Room

1. Introduction

In recent decades, rapid population growth, accelerated urbanization, and rising living standards have led to a significant increase in energy consumption in the building sector [1,2]. According to international reports, more than 40 % of global energy consumption is attributed to buildings, with a substantial portion devoted to heating, ventilation, and air conditioning (HVAC) systems [3,4]. The continuous growth in energy demand not only results in higher economic costs but also leads to serious environmental consequences, including increased greenhouse gas emissions and intensified climate change [5]. Recent life cycle assessment (LCA) studies across various sectors from transportation [6] to urban infrastructure [7] have increasingly highlighted the cumulative environmental footprint of energy-intensive systems, reinforcing the urgency of transitioning toward low-energy building technologies. Consequently, improving the efficiency of HVAC systems and developing innovative low-energy technologies have become key priorities for researchers and policymakers in the energy sector [8,9].

Indoor air quality and thermal comfort are among the most critical factors affecting human performance and productivity in enclosed environments. Parameters such as air temperature, relative humidity, air velocity, and particulate concentration play a direct role in determining occupants' thermal comfort [1]. An effective HVAC system must be capable of supplying adequate fresh air, removing pollutants, maintaining desired thermal conditions, and minimizing energy consumption [2]. In this context, the development of systems that ensure thermal comfort while reducing energy use is particularly important, especially in hot and dry climates. One such emerging technology is the radiant chilled ceiling system, which has gained considerable international attention in recent years [3–5] (Fig. 1).

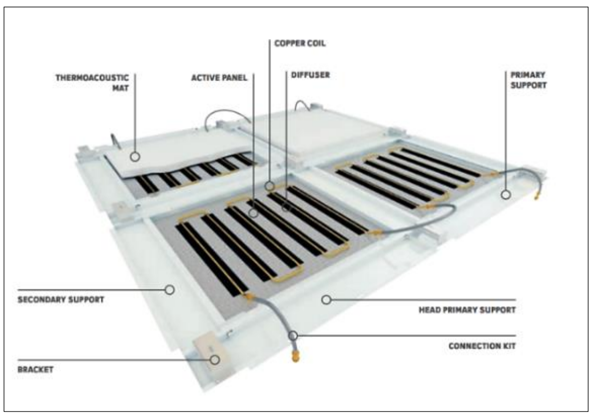

Fig. 1. Radiant ceiling panel [1]

In a chilled ceiling system, unlike conventional cooling systems that operate by directly blowing cool air, cooling is achieved indirectly through the creation of cold surfaces on the ceiling [1, 2]. These surfaces are typically kept cool by a hydraulic circuit consisting of chilled water pipes at a controlled temperature. Heat exchange between the space and the ceiling occurs through two main mechanisms: radiation and natural convection, with the radiative process accounting for approximately 50–55 % of this heat exchange. This characteristic enables the chilled ceiling system to provide more uniform thermal comfort with lower energy consumption compared to conventional systems [3–5].

From an implementation perspective, chilled ceiling systems can be categorized into several types. In some configurations, chilled water circulates through plastic pipes embedded in concrete ceilings, utilizing the thermal mass of the concrete to shift peak cooling loads to off-peak hours [8]. Another type employs flexible capillary tube networks installed within walls or gypsum ceilings, providing highly uniform temperature distribution [9]. The most common configuration is the panel-based system, consisting of metallic plates (typically aluminum) attached to chilled water pipes [10]. The use of materials with high thermal conductivity is crucial in these systems, as it enhances the responsiveness to thermal variations. In certain designs, air is also used as the working fluid [11].

Chilled ceiling systems offer several advantages due to their unique structure, including low energy consumption, reduced noise levels, uniform temperature distribution, lower airborne particulate concentration, and improved thermal comfort satisfaction [11–13]. Additionally, their relatively high operating temperature (approximately 16 °C) allows chillers to operate more efficiently, reducing overall energy consumption [12]. Compared to air-based systems, water pumps in these systems require only about 5 % of the energy consumed by fans, resulting in significant electricity savings [13]. Furthermore, these systems can be integrated with technologies such as free cooling, night cooling, and thermal energy storage, leading to peak load reduction and improved energy system stability [14]. In the broader context of urban water and energy sustainability, passive and low-energy approaches to resource management including innovative water collection strategies [15] serve as complementary directions for reducing the overall environmental burden of urban building systems.

Previous studies have shown that the thermal performance of chilled ceiling systems depends on various parameters, including the temperature difference between the surface and indoor air, material properties and thickness of the metal panel, pipe configuration, fluid flow rate, and insulation characteristics. For instance, Macáková et al. investigated the effects of geometric parameters and material properties of radiant ceiling panels on system performance, demonstrating that pipe spacing, pipe diameter, and panel thermal conductivity significantly influence cooling capacity [16]. Guo et al. conducted a numerical study on the performance of radiant ceiling systems combined with ceiling fans, showing that induced airflow improves temperature distribution and enhances heat transfer rates, partially compensating for the slow response of radiant systems [17].

Rasti and Salmanzadeh numerically analyzed the performance of radiant ceiling panels combined with radiant shields and ventilation air, concluding that radiant shields can reduce unwanted heat exchange and improve system efficiency, while ventilation air plays a key role in controlling panel surface temperature and preventing condensation [18].

Park and Chung examined the nominal cooling capacity of radiant ceiling panels under different building boundary conditions, highlighting the significant influence of environmental factors such as wall temperature, cooling load, and ventilation conditions on actual system performance [19].

In recent years, phase change materials (PCMs) have gained considerable attention in radiant ceiling applications. Boguto et al. evaluated a novel PCM-integrated radiant ceiling panel and reported enhanced thermal storage capacity, reduced surface temperature fluctuations, and improved system stability [20]. Rabani et al. experimentally investigated PCM application in ceiling cooling systems under the hot and dry climate of Yazd, demonstrating reduced energy consumption, improved thermal comfort, and decreased indoor temperature fluctuations, along with favorable economic feasibility [21]. Similarly, Liu et al., through numerical simulations, showed that integrating PCM into radiant systems enhances thermal stability and reduces temperature fluctuations, which is particularly important in sensitive environments [22].

Another study demonstrated that PCM with a melting temperature of 25 °C and a thickness of 74.2 mm provides optimal energy savings and reduces indoor temperature variations in hot and dry climates. The combination of PCM with night ventilation further improves cooling performance compared to conventional insulation [23].

Jobli et al. examined the effect of fluid flow rate on system performance and found that increasing the flow rate up to approximately 800 mL/min improves efficiency and system responsiveness [24]. Other studies have shown that a thin insulation layer enhances cooling capacity, whereas excessive insulation thickness has adverse effects [25].

Comparative analyses using TRNSYS indicate that aluminum panels outperform other materials in terms of cooling capacity and cost-effectiveness [26], while copper pipes improve performance due to their high thermal conductivity [27]. Additionally, an optimal aluminum plate thickness of approximately 0.7–1 mm has been suggested to balance performance and manufacturing cost [28].

Despite the breadth of existing research on radiant chilled ceiling systems, a critical review of the literature reveals several recurring methodological limitations. First, the majority of prior numerical studies have relied on two-dimensional or geometrically simplified models, which inherently cannot capture the three-dimensional temperature gradients, secondary flow structures in curved tube sections, or spatial non-uniformities in surface heat flux that arise under real panel operating conditions. For instance, the steady-state models employed by Ning et al. [27] and Ding et al. [28], while valuable for specific configurations, do not account for the transient thermal development that governs system start-up behavior and dynamic load response. Second, the parametric studies available in the literature have largely examined design variables in isolation: Jobli et al. [24] focused exclusively on the effect of mass flow rate, Ahmad and Lim [25] investigated only insulation thickness, and Macáková et al. [16] limited their analysis to geometric parameters without incorporating hydrodynamic coupling. This single-parameter approach precludes the identification of optimal design conditions that emerge from the interaction among geometric, thermal, and hydraulic variables interactions that are particularly significant in radiant ceiling panels operating under variable load conditions. Third, the transient behavior of metallic radiant panels, including the characteristic time required to reach thermal steady state and the evolution of temperature distribution during start-up, has received comparatively little systematic attention.

The present study addresses these gaps through a fully three-dimensional, transient numerical model developed in ANSYS Fluent, in which the coupled effects of pipe spacing, pipe diameter, mass flow rate, and inlet fluid temperature are simultaneously investigated within a single unified parametric framework. The transient formulation explicitly captures the thermal start-up dynamics of the panel, while the three-dimensional geometry faithfully resolves the flow behavior in the curved return sections and the spatial temperature distribution across the panel surface. The novelty of this work therefore lies in three distinct contributions: (i) the simultaneous, coupled investigation of four interdependent design parameters rather than sequential or isolated analyses enabling the identification of globally optimal operating conditions; (ii) the use of a transient, three-dimensional model that captures physical phenomena inaccessible to steady-state or simplified geometry approaches; and (iii) the systematic quantification of the laminar to turbulent flow transition and its disproportionate influence on cooling capacity, which has not been explicitly characterized in prior radiant ceiling panel studies. Together, these contributions establish a generalized numerical design framework that provides practically actionable, component level guidance for the development of energy efficient radiant cooling systems under diverse climatic and operational conditions.

2. Modelling

2.1. Geometry and boundary conditions

To determine the key parameters affecting the design of ceiling panels, the fluid flow inside copper tubes mounted on an aluminum plate was simulated using *ANSYS Fluent*. The objective of this modeling is to identify the optimal spacing between tubes, tube diameter, and the appropriate inlet mass flow rate. Accordingly, a preliminary model was developed as illustrated in Fig. 2, in which the spacing between the tubes is treated as a variable parameter.

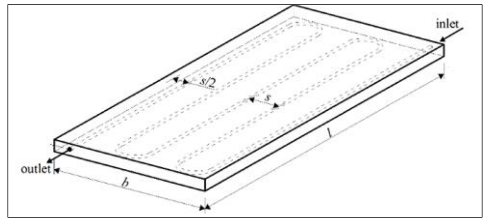

Fig. 2. Schematic of the initial modeling configuration

In this figure, s denotes the spacing between the tubes, l represents the length of the copper tubes, and b indicates the total width occupied by the tubes. In this model, two rows of U-shaped copper tubes are considered, as shown in Fig. 3. For the return sections, two 90° elbows with a radius of 0.1 m are employed [29].

In this problem, the boundary conditions are defined assuming unsteady, turbulent, incompressible flow with forced convective heat transfer of water inside the copper tubes. The inlet flow enters the tube with a temperature of T_i*=12-18 °C* and a uniform velocity u_i. The wall of the copper tube is divided into two semicircular regions (Fig. 4): the upper semicircle is assumed to be adiabatic (q = 0), representing the insulated back side of the panel facing the plenum or structural slab; the lower semicircle is subjected to a spatially uniform but operationally variable heat flux, $q = q(T_r, T_m)$, which is used to evaluate the cooling capacity. It should be noted that the term "constant heat flux" in this context refers to spatial uniformity along the surface at a given operating condition not a single fixed value applied identically across all parametric cases. For each parametric combination investigated in this study, the heat flux is recalculated based on the mean panel surface temperature T_m and the fixed room temperature T_r = 25 °C using the combined radiative convective formulation given in Eq. 4, which is adopted from BS EN 1264-2:2008+A1:2012 [30] the internationally recognized standard for the thermal performance evaluation of water-based surface-embedded cooling systems. This formulation simultaneously accounts for both long-wave radiative exchange and natural convective heat transfer between the panel surface and the conditioned space, providing a physically consistent boundary condition for the panel-level parametric analysis conducted herein. The tube length is assumed to be l*=1600 mm*.

Fig. 3. Sample of the modeled geometry used in the present study

In this study, the effects of tube spacing (s *= 0.05–0.3 m*), tube diameter (D *= 10-20 mm*), inlet mass flow rate of water (Q *= 0.005-0.045 kg/s*), and inlet temperature T_i on the heat flux generated at the lower semicircle of the copper tubes are investigated. A constant room temperature of 25 °C is assumed.

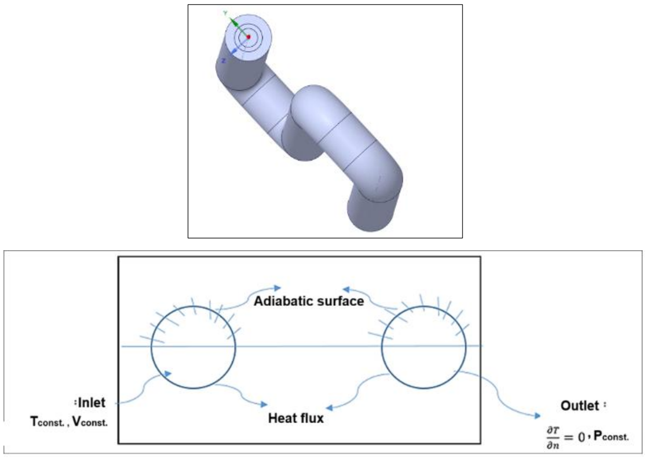

Fig. 4. Modeling of the copper tube wall and applied boundary conditions

2.2. Governing equations and solution method

The governing equations for a Newtonian, turbulent, unsteady, and incompressible flow consist of the continuity equation (Eq. 1), momentum equations (Eq. 2), and energy equation (Eq. 3), which are employed in the present study [31].

$$\frac{\partial \rho}{\partial t} + \frac{\partial(\rho u_i)}{\partial x_i} = 0 \quad (1)$$

$$\frac{\partial(\rho u_i)}{\partial t} + \frac{\partial(\rho u_i u_j)}{\partial x_j} = -\frac{\partial p}{\partial x_i} + \frac{\partial}{\partial x_j}\left[\mu\left(\frac{\partial u_i}{\partial x_j} + \frac{\partial u_j}{\partial x_i}\right)\right] + f_i \quad (2)$$

$$\frac{\partial(\rho i)}{\partial t} + \frac{\partial}{\partial x_j}\left[u_j(\rho i + P)\right] = \frac{\partial}{\partial x_j}\left[k\frac{\partial T}{\partial x_j}\right] + \Phi + S_h \quad (3)$$

For the present modeling, the pipe geometry is simulated in three dimensions. A no-slip boundary condition is imposed on all walls. A constant heat flux is applied on the lower semi-circular section of the wall, whereas the upper semi-circular surface is assumed to be thermally insulated. As mentioned earlier, the flow enters the pipe with uniform velocity and temperature, and a pressure outlet boundary condition is applied at the exit.

In this study, the pipe wall is modeled as two distinct semicircular sections: the upper semi-cylinder is treated as an adiabatic surface, while the lower semi-cylinder is subjected to a heat flux $q(T_r, T_m)$ that varies with the operating state of the panel. To simultaneously account for the combined effects of long-wave radiation and natural convection in the heat transfer between the panel surface and the indoor environment, the following formulation, adopted from BS EN 1264-2:2008+A1:2012 [30], is employed:

$$q = 8.92(T_r - T_m)^{1.1} \quad (4)$$

In this equation, T_r represents the fixed room air temperature (set to 25 °C throughout this study) and T_m denotes the mean surface temperature of the cooling panel, which is obtained from the numerical solution for each parametric case. Consequently, the applied heat flux is inherently coupled to the thermal state of the panel and is updated for each set of design parameters investigated, ensuring physical consistency across the parametric study. It is acknowledged that this panel-level formulation represents a simplification relative to a full room-level simulation that would incorporate spectrally resolved radiation transport and buoyancy driven convection of indoor air. However, this approach is consistent with established practice in the radiant ceiling panel literature [16, 27, 28] and is validated against experimental data from the ASHRAE Handbook (Fig. 8), confirming its adequacy for the purposes of the present parametric design study.

The numerical simulations are performed using ANSYS Fluent. A structured mesh is generated (Fig. 5), and the governing equations are solved using the finite volume method (FVM). In this approach, the computational domain is first discretized into a finite number of control volumes. The governing equations are then integrated over each control volume and transformed into a set of algebraic equations. To solve these equations, a pressure-based solver is employed, and the pressure–velocity coupling is achieved using the SIMPLEC algorithm. Furthermore, the second-order upwind scheme is utilized for the discretization of the momentum and energy equations. The convergence criterion for the present simulations is set to 10^{-7}.

In this study, the time step is determined based on the Courant number (Eq. 5) and its relation to the computational grid size. Considering the flow velocity, mesh element dimensions, and to ensure numerical stability and accuracy, a time step of 0.02 s is selected. Moreover, due to the use of an implicit scheme in transient modeling, stable and proper convergence of the governing equations is achieved, allowing the use of this time step without numerical instability. This selection provides an appropriate balance between solution accuracy and computational cost.

$$Co = \frac{u \Delta t}{\Delta h} \quad (5)$$

2.3. Mesh-independent solution

To demonstrate the grid independence of the numerical results, the outlet fluid temperature was computed for five progressively refined mesh configurations, and the results are presented in Fig. 6. As observed, the outlet temperature decreases monotonically with mesh refinement and reaches a plateau beyond a certain threshold. Specifically, the relative change in outlet temperature between successive mesh levels decreases from 1.8% (between Mesh 2 and Mesh 3) to 0.31% (between Mesh 3 and Mesh 4), and further to 0.08% (between Mesh 4 and Mesh 5), confirming convergence. On this basis, a mesh consisting of 313,500 elements was selected as the optimal configuration, beyond which further refinement yields changes smaller than 0.1% in the monitored variable a threshold widely accepted as the criterion for mesh independence in engineering CFD studies.

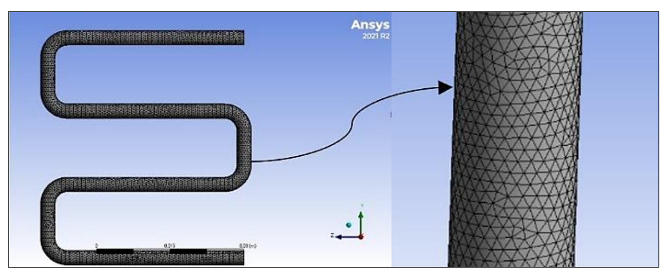

Fig. 5. Mesh generation of the cooling system in ANSYS software

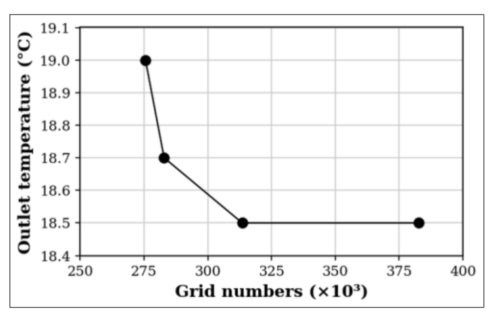

Fig. 6. Effect of mesh refinement on the outlet temperature of the copper tube

In addition, a refined near-wall mesh was employed to accurately resolve the viscous sublayer and capture boundary layer effects without the use of empirical wall functions. The computational grid was designed such that the dimensionless wall distance y^+ remains approximately equal to 1 throughout the domain. The spatial distribution of y^+ along the tube length is presented in Fig. 7, confirming that its value remains consistently below 1.3 across the entire wall surface, with a mean value of approximately 0.85. This near-wall resolution is consistent with the requirements of the SST k–ω turbulence model employed in this study, which requires $y^+ \leq 1$ for accurate near-wall treatment without wall functions.

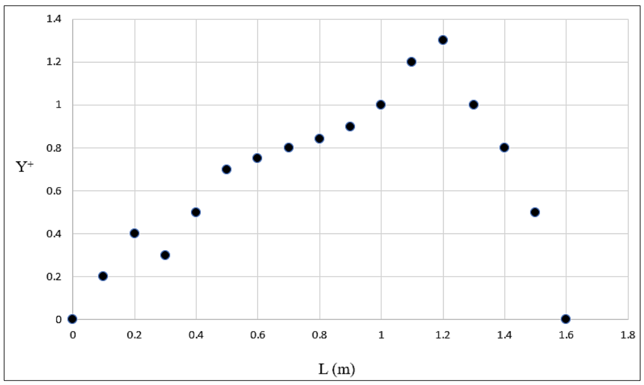

Fig. 7. Variation of y^+ along the tube length

2.4. Problem Validation

Prior to conducting the parametric study, the accuracy and reliability of the numerical model were rigorously verified through a systematic validation procedure involving comparison of the present simulation results against two independent reference datasets: (i) the experimental correlations for radiant ceiling cooling panels reported in the ASHRAE Handbook HVAC Systems and Equipment [32], which constitutes the most widely adopted international benchmark for panel-level thermal performance evaluation, and (ii) the numerical results reported by Ning et al. [27], whose study employed a comparable geometric configuration and boundary condition framework.

The validation was carried out for a representative base-case configuration with the following boundary conditions, selected to match those reported in the ASHRAE reference: an inlet water temperature of T_i = 15 °C, a fixed room air temperature of T_r = 25 °C, a mean water velocity of U = 0.2 m/s (corresponding to a mass flow rate of Q = 0.016 kg/s), a pipe inner diameter of D = 12 mm, a tube length of l = 1600 mm, and a center-to-center tube spacing of s = 0.15 m. The lower semicircular surface of the tube was subjected to the combined radiative convective heat flux defined by Eq. 4, yielding a heat flux of approximately q = 62 W/m² under the specified conditions. The upper semicircular surface was treated as adiabatic, consistent with the standard panel-level modeling approach described in Section 2.1.

The comparison between the numerically predicted cooling capacity and the ASHRAE reference values is presented in Fig. 8 as a function of the mean panel surface temperature T_m, over a range of T_m from 14 °C to 20 °C. As observed in Fig. 8, the numerical results are in close agreement with the experimental ASHRAE data across the entire temperature range considered, with a maximum absolute deviation of 2.4% and a mean absolute percentage error (MAPE) of 2.2%, both of which fall within the accepted tolerance for engineering CFD validation studies. The cooling capacity increases monotonically as T_m decreases relative to the fixed room temperature, consistent with the driving temperature difference in Eq. 4. The slight overestimation observed at lower values of T_m (i.e., T_m < 15 °C) is attributed to the assumption of uniform heat flux along the lower semicircle, which tends to marginally overpredict the effective panel-to-room heat exchange at high temperature differentials. This systematic offset remains within 2.3% and does not affect the validity of the comparative parametric analysis.

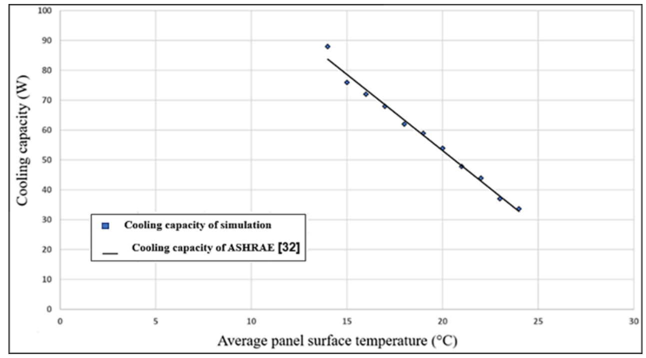

Fig. 8. Validation of the present work with experimental data provided in the ASHRAE Systems and Equipment Handbook [32]

Furthermore, a comparison with the numerical results of Ning et al. [27] under identical boundary conditions confirms that the present model predicts cooling capacity values within 4% of those reported in that study, providing additional confidence in the accuracy of the adopted mesh configuration and turbulence model. It is noted that the mesh employed in this validation case is the same as that selected through the mesh independence study described in Section 2.3 (mesh density of 313,500 elements, yielding a maximum y^+ value of approximately 1 on the tube wall), ensuring that the agreement observed here is not contingent on mesh refinement beyond the converged configuration. Taken together, these results confirm that the present numerical framework accurately reproduces the thermal performance of radiant ceiling panels under the conditions of interest, and that it constitutes a reliable basis for the systematic parametric investigation presented in Section 3.

3. Results

3.1. The effect of spacing between tubes

After determining an appropriate mesh, the investigated panel was modeled, and the resulting temperature distribute on for a representative loop of the panel is shown in Fig. 9. consistent with the boundary conditions described in Section 2.1. The inlet flow into the copper tubes is modeled at a constant velocity and a temperature of 15 °C, while the outlet is defined as a pressure outlet. Based on the conducted studies, the initial inner diameter of the copper tube is assumed to be 12 mm, and the water velocity is set to 0.2 m/s. Fig. 9 illustrates the significance of the tube spacing in preventing vortex formation at the curved sections of the pipe, thereby ensuring a more uniform temperature distribution across the entire panel.

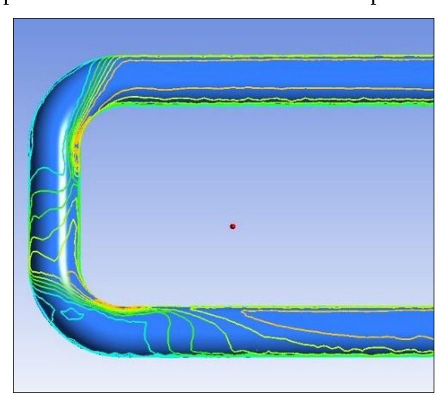

Fig. 9. Temperature distribution in one loop of the ceiling panel

As can be observed, the spacing between the tubes has a significant impact on suppressing vortex formation in the curved regions of the pipe and consequently on achieving a uniform temperature distribution throughout the panel. Therefore, the effect of tube spacing in the ceiling panel is first investigated.

Fig. 10 shows that the spacing between the tubes has a considerable influence on the cooling capacity of the panel. The tube spacing within the feasible range of 0.05 to 0.30 m was varied linearly with a step of 0.05 m; yielding six cases in total, all of which are shown in Fig. 10. With increasing tube spacing, the cooling capacity decreases uniformly. Therefore, although a spacing of 0.05 m provides the highest cooling performance, considering practical constraints and installation feasibility, a range of 0.10 to 0.15 m can be selected as an optimal and practical design choice. In fact, reducing the tube spacing increases the effective radiative heat transfer area, thereby enhancing the cooling capacity.

Reducing the tube spacing to less than 10 cm leads to an increase in the total pipe length over a given surface area, and consequently increases the number of joints and installation complexity, which significantly raises the construction and installation costs of the system. In addition, higher pipe density results in increased pressure losses in the flow circuit, leading to higher pump power consumption and operating costs. From an implementation standpoint, the minimum bending radius limitation of copper tubes also makes excessive reduction in spacing more difficult to implement, increasing the risk of mechanical stress, cracking, or damage to the tubes. Therefore, selecting a spacing of less than 10 cm, despite its slight thermal performance improvement, is not justified from technical and economic perspectives.

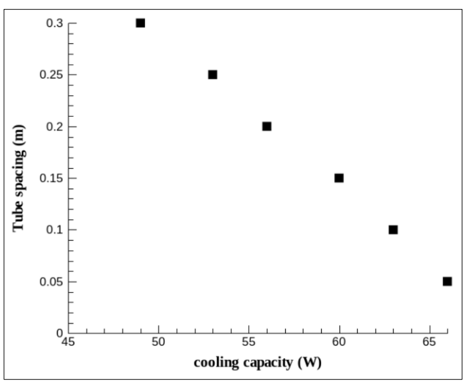

Fig. 10. Effect of tube spacing on cooling capacity

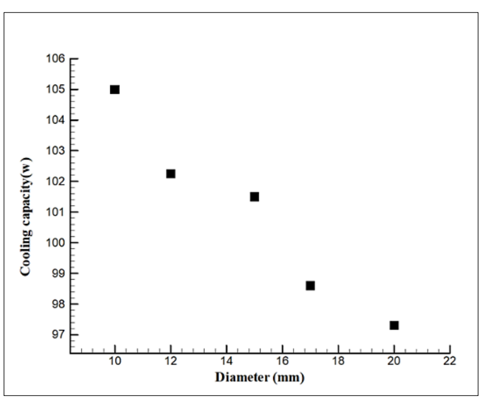

Fig. 11. Effect of copper tube diameter on the cooling capacity of the panel

3.2. The effect of pipe diameter

To investigate the effect of the copper tube diameter on the cooling capacity of the panel, tube diameters within the available range of 10 to 20 mm were analyzed with a step of 1 mm, yielding eleven simulated cases. To keep the figure legible given how closely spaced the results are, five representative diameters are shown in Fig. 11. It should be noted that the water flow rate was kept constant in all cases.

Given the inverse relationship between flow velocity and tube cross-sectional area, a reduction in diameter leads to an increase in flow velocity and, consequently, an enhancement in cooling capacity. Therefore, from a thermal performance perspective, smaller diameters are considered more optimal; however, due to manufacturing and implementation constraints, a diameter of 12 mm was selected as the most suitable option.

The use of smaller tube diameters, according to the Darcy–Weisbach relation, results in a significant increase in frictional pressure losses along the flow path, since the pressure drop is inversely proportional to the pipe diameter and directly proportional to the square of the flow velocity. Consequently, to maintain a constant mass flow rate, reducing the tube diameter increases fluid velocity and frictional losses, thereby imposing a higher pumping power requirement on the system. Accordingly, the selection of tube diameter in the design of radiant ceiling panels is always made as a trade-off between enhanced heat transfer performance and limiting pump power consumption.

3.3. The effect of water flow rate

To investigate the effect of water flow rate, the cooling capacity was calculated using 40 different values of inlet water mass flow rate in the copper tubes, ranging from 0.005 to 0.045 kg/s with an increment of 0.001 kg/s. For clarity, 14 representative flow rates spanning the laminar-to-turbulent transition are plotted in Fig. 16. The effect of inlet flow rate on the flow distribution inside the tube is shown in Figs. 12-15.

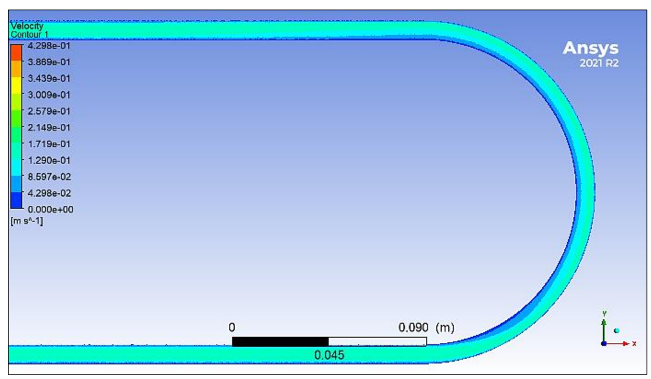

Fig. 12. Effect of inlet flow rate on flow distribution inside the tube for an inlet mass flow rate of 0.010 kg/s

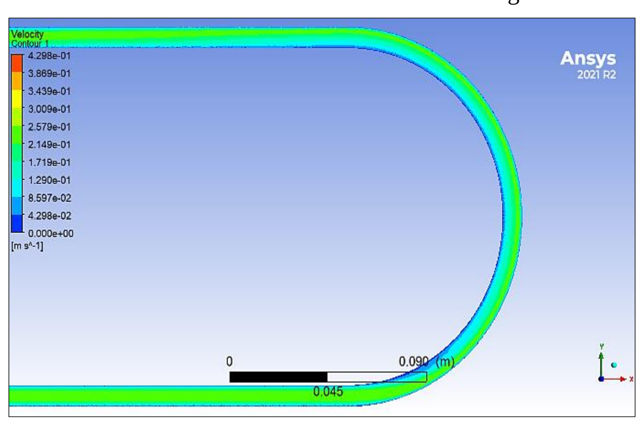

Fig. 13. Effect of inlet flow rate on flow distribution inside the tube for an inlet mass flow rate of 0.015 kg/s

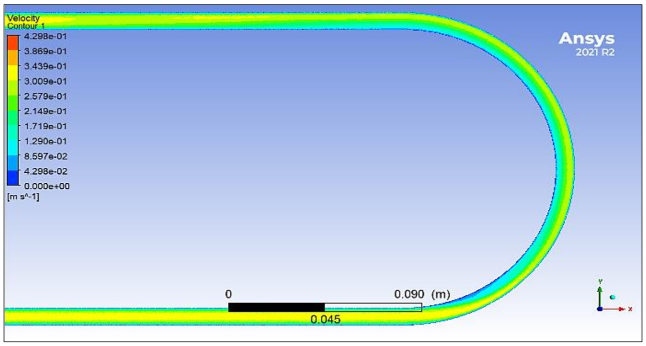

Fig. 14. Effect of inlet flow rate on flow distribution inside the tube for an inlet mass flow rate of 0.016 kg/s

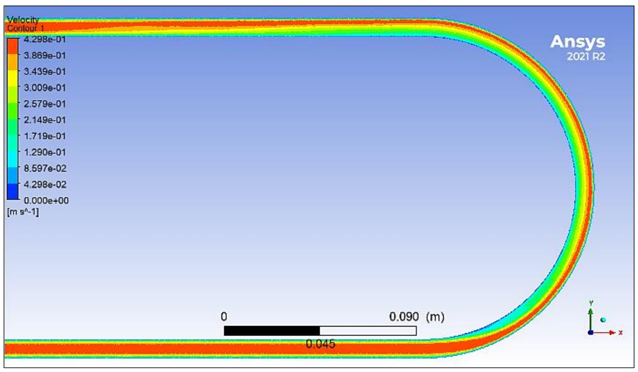

Fig. 15. Effect of inlet flow rate on flow distribution inside the tube for an inlet mass flow rate of 0.017 kg/s

As observed, increasing the mass flow rate leads to an increase in flow velocity. As the flow regime approaches the turbulent region, the development of vortex structures and the intensity of velocity fluctuations become clearly evident. This increase in turbulence enhances the mixing process, results in a more uniform temperature distribution across the flow cross-section, reduces the fluid-side thermal resistance, and consequently improves the cooling capacity of the system. This trend is clearly illustrated in Fig. 16.

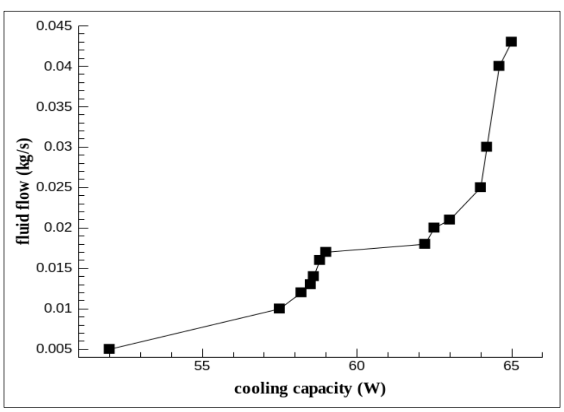

Fig. 16. Effect of flow rate on cooling capacity

As shown in Fig. 16, by increasing the mass flow rate from 0.016 kg/s to 0.017 kg/s, a noticeable jump in cooling capacity occurs. This change is primarily attributed to the transition from laminar to turbulent flow regime. After the flow enters the turbulent region, further increases in mass flow rate lead to a gradual and relatively smooth improvement in cooling capacity. Since the stability of the turbulent regime plays a key role in the thermal performance of the system, the selection of the optimal flow rate should ensure that the flow reliably remains within the turbulent regime.

3.4. The effect of inlet water temperature

One of the key parameters in the design of radiant cooling systems is the determination of the working fluid inlet temperature to the panel. Since the inlet temperature has a direct impact on the cooling capacity, heat transfer performance, and prevention of condensation on the panel surface, its selection is of particular importance. In this study, considering operational requirements and environmental constraints, the water inlet temperature to the ceiling cooling panel was selected in the range of 12 to 18 °C with 1 °C increments. The effect of this parameter on the cooling capacity is presented in Fig. 17.

Maintaining the water inlet temperature within the range of 12–18 °C is associated with several challenges, including variations in ambient temperature, fluctuations in the space cooling load over a diurnal cycle, and changes in system operating conditions. These factors may lead to instability in the chilled water outlet temperature from the chiller and consequently alter the performance of the radiant ceiling panels. Therefore, achieving a stable inlet temperature within this range requires the implementation of precise control strategies and system-level intelligent management to ensure safe, stable, and efficient operation.

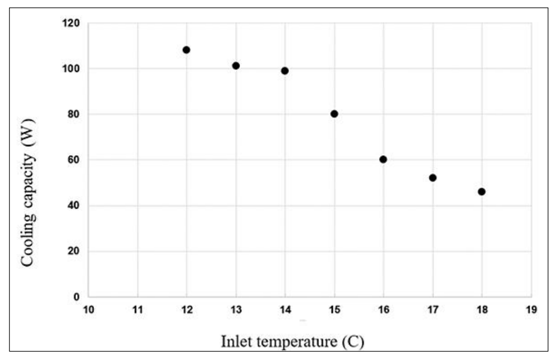

Fig. 17. Effect of inlet temperature in copper tubes on cooling capacity

As illustrated in Fig. 17, this temperature range ensures not only satisfactory thermal performance but also safe and stable system operation. Based on the presented results, an inlet temperature of 15 °C is identified as the optimal condition, as it provides adequate cooling capacity while also representing a cost-effective operating point from an economic perspective.

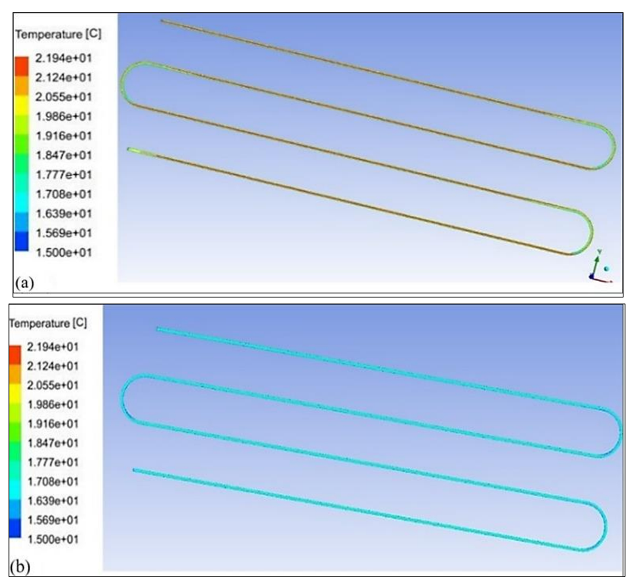

Fig. 18. Temperature distribution after (a) 1 minute and (b) 3 minutes of operation

In addition to the steady-state parametric analyses presented above, a transient simulation was carried out to characterize the thermal start-up behavior of the panel system. Since the computational domain consists solely of a copper tube ($k \approx 387$ W/m·K) and a thin aluminum plate ($k \approx 202$ W/m·K), both materials of high thermal conductivity and inherently low thermal mass, the system is expected to reach a quasi-steady thermal state within a few minutes of start-up. This expectation is further supported by the hydraulic residence time of the fluid inside the tube, which given the tube length of l = 1600 mm and the mean fluid velocity of u = 0.2 m/s is approximately 8 seconds. Accordingly, the transient simulation was conducted for a total physical duration of 3 minutes, using a time step of Δt = 0.02 s, corresponding to 9,000 time steps in total a computationally rational configuration consistent with the thermal characteristics of the model.

The temperature distribution within the tube network at two representative time instants, t = 1 min and t = 3 min, is shown in Fig. 18. As observed in Fig. 18, the temperature field evolves progressively during the first minute of operation. At t = 1 min, the temperature distribution has not yet reached a fully developed and spatially uniform pattern, particularly near the inlet region and the return bends. However, by t = 3 min, both the temperature distribution across the panel surface and the associated cooling capacity have stabilized to a near-steady condition, confirming that the thermal response time of this panel configuration is on the order of a few minutes. This rapid thermal equilibration is a notable practical advantage of metallic radiant ceiling panels compared to thermally massive systems such as concrete-embedded piping, in which equilibration may require several hours. The use of an implicit time-integration scheme ensures numerical stability across all time steps, and the convergence criterion of 10^{-7} was satisfied at each time step throughout the transient simulation.

4. Limitations and Future Studies

4.1. Limitations of the Present Study

While the numerical framework developed in this study provides a systematic and validated basis for the parametric design of radiant ceiling panels, several inherent limitations should be acknowledged to guide the interpretation of results and to define the scope of future investigations.

First, the computational domain is intentionally restricted to the panel level, comprising only the copper tube and the aluminum plate. Consequently, the model does not account for the full room level thermal environment, including long-wave radiation exchange between the panel and the surrounding enclosure surfaces, buoyancy-driven natural convection of indoor air, dynamic interaction with occupants and internal heat gains, or the influence of ventilation airflow on panel performance. A full room level multi-physics simulation incorporating a radiation transport model (e.g., the Discrete Ordinates or Surface to Surface method) coupled with a turbulence model for indoor airflow would more faithfully represent the actual operating environment of a radiant cooling panel, at the cost of substantially greater computational effort.

Second, the thermal boundary condition applied to the lower semicircle of the tube wall is derived from the combined radiative convective formulation of BS EN 1264-2:2008+A1:2012 [30], which, while physically consistent and widely adopted in the radiant panel literature, represents a simplification of the true coupled heat exchange process. In particular, this formulation assumes a spatially uniform combined heat transfer coefficient and does not resolve the local variation in convective and radiative contributions across the panel surface.

Third, the thermophysical properties of the working fluid (water) are assumed constant throughout the simulation. In practice, these properties particularly dynamic viscosity and thermal conductivity exhibit temperature dependence that may become significant when the temperature differential between the inlet and outlet is large, or when operation near the dew point is considered.

Fourth, the present model does not incorporate condensation risk prediction. While the inlet temperature range of 12–18 °C was selected in part to mitigate condensation risk, a dedicated psychrometric model coupled with surface temperature prediction would be necessary to quantify condensation probability under variable indoor humidity conditions.

4.2. Directions for Future Studies

The limitations identified above suggest several productive directions for extending the present work.

- Room level and building scale modeling: Future studies should progressively expand the computational domain to incorporate full room level CFD, coupling the panel model with radiation transport, buoyancy-driven airflow, and occupant thermal models. Integration with building energy simulation platforms such as EnergyPlus or TRNSYS would further enable the evaluation of radiant ceiling systems over annual operational cycles and under diverse climatic conditions, providing a more complete basis for lifecycle energy assessment.

- Phase change material (PCM) integration: As demonstrated in recent studies [20–23], PCM integration represents one of the most promising directions for enhancing the thermal storage capacity and load-shifting potential of radiant ceiling panels. Future numerical work should investigate the coupled optimization of PCM properties (melting temperature, thickness, thermal conductivity) and panel geometry parameters within the framework established in the present study.

- Integration with artificial intelligence and machine learning techniques: Perhaps the most transformative direction for future research lies in the integration of the present numerical framework with data-driven modeling approaches. Recent advances have convincingly demonstrated the capability of artificial neural networks and machine learning algorithms to predict, optimize, and control the performance of complex thermodynamic and energy systems. For example, the application of neural networks to the optimization of heat recovery from gas turbine exhaust for absorption chiller operation has shown that data-driven models can accurately predict system efficiency across a wide range of operating conditions while substantially reducing the computational burden associated with full numerical simulations [33]. Similarly, a systematic comparative study of supervised and unsupervised machine learning models applied to energy systems has established that ensemble methods, support vector regression, and deep neural networks consistently outperform classical empirical correlations in capturing the nonlinear relationships between design variables and system performance metrics [34]. These findings are directly applicable to the radiant ceiling panel context, where the coupled nonlinear dependence of cooling capacity on pipe spacing, diameter, flow rate, and inlet temperature as characterized in the present study constitutes precisely the type of multi-dimensional input–output mapping for which machine learning models are most effective.

In this context, the numerical dataset generated by the present parametric study (spanning 40 mass flow rate values, multiple diameters, spacings, and inlet temperatures) provides a high-quality training corpus that could support the development of surrogate models capable of near-instantaneous performance prediction, real-time optimization, and model predictive control of radiant cooling systems in building automation frameworks. Furthermore, the accuracy of statistical and machine learning forecasting models across diverse energy and environmental indicators including emissions trajectories and sustainability metrics has been established in recent comparative analyses [35], supporting the feasibility of embedding such predictive tools within the lifecycle sustainability assessment of low-energy cooling technologies.

Future work should therefore focus on: (i) training deep neural network surrogate models on extended numerical datasets generated by the present framework; (ii) embedding these surrogate models within multi-objective optimization algorithms (e.g., genetic algorithms or Bayesian optimization) to identify Pareto-optimal design configurations under competing objectives such as cooling capacity, condensation risk, and pumping energy; and (iii) integrating the resulting models with building management systems for dynamic, data-driven control of radiant ceiling panel operation under variable occupancy and climatic conditions.

5. Conclusions

In this study, a numerical simulation of chilled water flow in copper tubes attached to an aluminum plate was performed using ANSYS Fluent in order to analyze and optimize the performance of radiant ceiling panels. The results indicate that the thermal performance of radiant cooling ceiling systems is directly influenced by geometric parameters and fluid flow conditions. Tube spacing, tube diameter, flow rate, and inlet fluid temperature were identified as the most significant factors affecting cooling capacity and the uniformity of temperature distribution. It was also shown that even minor variations in these parameters can lead to considerable changes in the overall performance of the panel, highlighting the importance of accurate design.

The analysis of geometric parameters demonstrates that reducing tube spacing enhances cooling capacity; however, practical limitations and installation costs must be considered simultaneously. In this regard, a spacing range of 10 to 15 cm is proposed as an optimal compromise, providing a balanced trade-off between cooling performance, surface temperature uniformity, and constructability. The investigation of tube diameter further reveals that although reducing the diameter increases flow velocity and improves heat transfer, excessively small diameters are not feasible from a manufacturing and installation perspective. Therefore, a tube diameter of 12 mm is recommended as an appropriate choice.

The flow condition analysis shows that increasing the flow rate leads to a transition toward turbulent flow, enhanced fluid mixing, and a more uniform temperature distribution, resulting in a significant improvement in cooling capacity. After entering the turbulent regime, further increases in flow rate have a more gradual effect on system performance. The results also indicate that selecting an inlet water temperature in the range of 12 to 18 °C provides adequate cooling capacity while preventing condensation. The transient analysis further confirms that the system reaches a steady thermal state after a certain period of operation.

The parameter optimization presented in this study offers practical, component-level design guidance namely tube spacing, diameter, flow rate, and inlet temperature for a single radiant ceiling panel loop. Extending this analysis toward building-scale applications, in which multiple panels are dynamically coordinated through intelligent flow and temperature control to accommodate variable occupancy and thermal loads in large or sensitive facilities such as hospitals and healthcare centers, represents a promising direction for future work. Realizing this extension, however, would require network-level and multi-zone simulations beyond the single-loop, isolated-boundary-condition model presented here.

It should be noted that the present numerical framework operates at the panel level, with the thermal boundary condition on the outer surface of the tube formulated according to BS EN 1264-2:2008+A1:2012 [30], which provides a combined representation of radiative and natural convective heat exchange between the panel and the conditioned space. While this approach is physically consistent and validated against ASHRAE experimental data, it represents a simplification relative to full room-level simulations incorporating coupled radiation transport, buoyancy-driven indoor air convection, and dynamic interaction with surrounding surfaces. Future studies incorporating such room-level multi-physics models would further extend the generalizability of the present results to more complex and realistic building configurations.

References

[1] S. A. Mumma, "Ceiling Panel Cooling Systems", *ASHRAE Journal*, vol. 43, pp. 28–32, 2001.

[2] J. Dieckmann, K. W. Roth, and J. Brodrick, "Radiant Ceiling Cooling", *ASHRAE Journal*, vol. 46, pp. 68–70, 2004.

[3] R. A. Meierhans, "Room Air Conditioning by Means of Overnight Cooling of the Concrete Ceiling", *ASHRAE Transactions*, vol. 102, pp. 693–697, 1996.

[4] L. Ferkl and J. Syroky, "Ceiling Radiant Cooling: Comparison of ARMAX and Subspace Identification Modelling Methods", *Building and Environment*, vol. 45, pp. 205–212, 2010.

[5] K. A. Antonopoulos, M. Vrachopoulos, and C. Tzivandis, "Experimental and Theoretical Studies of Space Cooling Using Ceiling-Embedded Piping", *Applied Thermal Engineering*, vol. 17, pp. 351–367, 1997.

[6] M. A. Shirazi, R. Zahedi, H. Yousefi and A. Aslani, "Environmental and damage assessment of electric vehicles compared to internal combustion engine vehicles under various ambient temperature scenarios using the LCA approach", *Energy Nexus*, vol. 20, pp. 100606, 2026.

[7] M. Moaven, M. A. Shirazi and M. H. Ghodusinejad, "Systematic Analysis of the Impact of Life Cycle Assessment of Materials on Urban Heat Island Mitigation: A Path Toward Sustainable Urban Policy Using the PRISMA Method", *Urban Development Policy Making*, vol. 2, pp. 95–110, 2025.

[8] P. Jacobs, E. C. van Oeffelen, and B. Knoll, "Diffuse Ceiling Ventilation: A New Concept for Healthy and Productive Classrooms", TNO Built Environment and Geosciences, Delft, The Netherlands, Tech. Rep., 2008.

[9] C. A. Hviid and S. Svendsen, "Experimental and Numerical Analysis of Perforated Suspended Ceiling as Diffuse Ventilation Air Inlets", in *Proceedings of Room vent Conference*, 2009.

[10] C. A. Hviid and S. Terkildsen, "Experimental Study of Diffuse Ceiling Ventilation in a Classroom", Technical University of Denmark, 2010.

[11] T. Mikeska and J. Fan, "Full-Scale Measurements and CFD Simulations of Diffuse Ceiling Inlet for Ventilation and Cooling of Densely Occupied Rooms", *Energy and Buildings*, vol. 68, pp. 1–8, 2014.

[12] K. A. Antonopoulos and C. Tzivandis, "Numerical Solution of Unsteady Three-Dimensional Heat Transfer During Space Cooling Using Ceiling-Embedded Piping", *Energy*, vol. 22, pp. 59–67, 1997.

[13] M. Tye-Gingras and L. Gosselin, "Comfort and Energy Consumption of Hydronic Heating Radiant Ceiling and Walls Based on CFD Analysis", *Building and Environment*, vol. 54, pp. 1–13, 2012.

[14] S. Moslehi, M. Maerefat, and R. Arababadi, "Engineering and Construction Applicability of Radiant Heating-Cooling Ceiling Panels in Residential Buildings in Different Climates of Iran", *Procedia Engineering*, vol. 145, pp. 18–25, 2016.

[15] M. A. Shirazi, H. Yousefi, A. Fathi and M. Baneshi, "Urban Water Sustainability through Energy-Free Fog Water Harvesting: A Review of Fog-Collecting Systems", *Urban Development Policy Making*, vol. 3, pp. 69–94, 2025.

[16] L. Macáková, R. Lenhard, and K. Kaduchová, "Influence of Geometric and Material Parameters on the Performance of Radiant Ceiling Cooling Systems", in *42nd Annual Conference*

of the Departments of Fluid Mechanics and Thermomechanics, vol. 412, 2025.

[17] X. Guo, S. Wan, W. Chen, H. Zhang, E. Arens, Y. Cheng, and W. Pasut, "Numerical Simulation of Cooling Performance of Radiant Ceiling System Interacting with a Ceiling Fan", *Energy and Buildings*, vol. 297, pp. 113492, 2023.

[18] F. Rasti and M. Salmanzadeh, "Numerical Evaluation of the Thermal Performance of a Ceiling Radiant Cooling Panel Integrated with Radiation Shields and Ventilation Air", *Journal of Building Engineering*, vol. 99, pp. 111688, 2025.

[19] S. P. Park and W. J. Chung, "Evaluation of Nominal Cooling Capacity of Ceiling Radiant Panels Under Varying Building Boundary Conditions", *Journal of Building Engineering*, vol. 101, pp. 111723, 2025.

[20] D. I. Bogatu, J. Shinoda, B. W. Olesen, and O. B. Kazanci, "Cooling Performance Evaluation of a Novel Radiant Ceiling Panel Containing Phase Change Material (PCM)", *Journal of Building Engineering*, vol. 103, pp. 112051, 2025.

[21] M. Rabani, M. Alafzadeh, and M. Rabani, "Performance Evaluation of Ceiling Cooling with PCM in the Hot-Dry Climate of Yazd, Iran: An Experimental Analysis of Energy, Environmental, and Economic Impacts", *Buildings*, vol. 15, pp. 198, 2025.

[22] H. Liu, X. Li, S. Liu, H. Zhang, Z. Han, and B. Gao, "Simulation Study on Suppressing Temperature Fluctuation Based on PCM for Radiant Supply Cooling Systems in Thermodynamic Measurement Laboratory", *Building Simulation*, vol. 18, pp. 2275–2291, 2025.

[23] M. Alafzadeh and M. Rabani, "Numerical Analysis of the Impact of Phase Change Materials on the Optimization of Building Cooling Load", *Energy Engineering and Management*, vol. 14, pp. 52–65, 2025.

[24] M. I. B. Jobli, R. Yao, Z. Luo, M. Shahrestani, N. Li, and H. Liu, "Numerical and Experimental Studies of a Capillary-Tube Embedded PCM Component for Improving Indoor Thermal Environment", *Applied Thermal Engineering*, vol. 148, pp. 466–467, 2019.

[25] N. A. Ahmad and C. W. Lim, "Simplified Model and Performance Analysis for Radiant Cooling Panel with Serpentine Tube Arrangement and Thin Insulation Layer for Moisture Control in Tropical Climate", *Journal of Physics: Conference Series*, vol. 1522, 2020.

[26] Y. Mori and W. Nakayama, "Study of Forced Convective Heat Transfer in Curved Pipes (2nd Report, Turbulent Region)", *International Journal of Heat and Mass Transfer*, vol. 10, pp. 37–59, 1967.

[27] B. Ning, Y. Chen, H. Liu, and S. Zhang, "Cooling Capacity Improvement for a Radiant Ceiling Panel with Uniform Surface Temperature Distribution", *Building and Environment*, vol. 102, pp. 64–72, 2016.

[28] L. Ding, T. Katsura, A. Radwan, and K. Nagano, "Thermal Performance Analyses of a New Multi-Segmented Minichannel-Based Radiant Ceiling Cooling Panel", *Energy Reports*, vol. 6, pp. 1409–1415, 2020.

[29] G. Cammarata, G. Petrone, and F. Masi, "Numerical Simulation of Radiant Ceiling Panels for Indoor Cooling", *Journal of Physics: Conference Series*, vol. 655, 2015.

[30] Water Based Surface Embedded Heating and Cooling Systems - Part 2: Floor Heating: Prove Methods for the Determination of the Thermal Output Using Calculation and Test Methods, BS EN1264-2:2008+A1:2012, May 31, 2009.

[31] M. Rabani, "Performance Analysis of a Passive Cooling System Equipped with a New Designed Solar Chimney and a Water Spraying System in an Underground Channel", *Sustainable Energy Technologies and Assessments*, vol. 35, pp. 204–219, 2019.

[32] *ASHRAE Handbook - HVAC Systems and Equipment (SI)*, Chapter 6: Panel Heating and Cooling, American Society of Heating, Refrigerating and Air-Conditioning Engineers Inc., Atlanta, GA, 2008.

[33] A. Naziri, A. R. Tahavvor, M. A. Shirazi, and R. Zahedi, "Feasibility study on heat recovery from gas turbine exhaust for absorption chiller operation and efficiency enhancement using neural networks", *Thermal Science and Engineering Progress*, vol. 67, pp. 104210, 2025.

[34] A. Saifoddin, N. Mirzaei, M. A. Shirazi, and H. Yousefi, "Comparative Applications of Supervised and Unsupervised Machine Learning Models in Energy Systems", *Journal of Energy Management and Technology*, vol. 9, pp. 284–290, 2025.

[35] S. M. Moezzi, M. A. Shirazi, A. Rajabi, Z. Monfared, and H. Yousefi, "Comparison of classical statistical models for forecasting CO_2 emissions, GDP, and TBL cancer indicators: A comparative analysis of East and West Asia", *Energy Nexus*, vol. 21, pp. 100682, 2026.